

## Growth and Characterization of Germanium-based type I Clathrate Thin Films Deposited by Pulsed Laser Ablation

S. Witanachchi, R. Hyde, H. S. Nagaraja, M. Beekman, G. S. Nolas, and P. Mukherjee  
Department of Physics, University of South Florida, Tampa, FL 33620

### ABSTRACT

Thin films of clathrate material have been grown using the laser ablation technique on a variety of substrates. Films deposited on silicon substrates exhibited a significant deficiency of Ga and Ge while the stoichiometry was preserved in films deposited on quartz, sapphire, and glass substrates. Ablation characteristics of the clathrate target for laser radiation at three different wavelengths in the UV, visible and IR were studied. The UV and IR laser wavelengths produce low ablation thresholds and high growth rates. Crystalline films were obtained above a growth temperature of 400°C. Conductivity measurements on the films at low current injection (<40  $\mu$ A) showed semiconducting behavior. At high currents the films demonstrated a semiconductor-to-metal transition for temperatures lower than 150 K.

### INTRODUCTION

Several new approaches are currently being pursued in the search for novel thermoelectric materials. [1] One of these approaches, first proposed by Slack [2], is to find materials which operate as so-called “phonon-glass electron-crystals” (PGEC). Such PGEC materials would possess electronic properties similar to a good single-crystal semiconductor, yet impede thermal transport in a manner similar to a structural glass. This approach has proven very useful in the search for new thermoelectric materials, in particular by the progress made with skutterudite compounds [3, 4]. Slack also suggested [5] that the class of materials known as clathrates might fulfill many of the PGEC requirements, and Nolas et al. first showed that these materials indeed comprise potential candidates for thermoelectric applications [6].

Inorganic clathrates were first systematically investigated by Cros et al. in the 1960 s [7], and possess structures analogous to the gas or clathrate hydrates. Type I inorganic clathrates are characterized by a framework composed typically of Group IV elements, which occupy sites at the vertices of face-sharing polyhedra, two tetrakaidecahedra and six pentagonal dodecahedra per cubic unit cell. Guest atoms in turn occupy the crystallographic sites found inside these polyhedra, and a general chemical formula for type I clathrates can be written as  $A_8X_yY_{46-y}$ , where A represents the guest atom, and X and Y represent the Group IV or substituting framework atoms.

Since the initial reports showing promising thermoelectric properties in type I clathrates [6], active investigations into the properties of these materials have been undertaken by numerous groups. Some type I clathrates show a truly “glasslike” thermal conductivity [8], explained in terms of the unique guest-framework interaction in these structures. The loosely bound guests in these crystalline materials can undergo large, localized low-frequency vibrations, which in turn can scatter the heat-carrying acoustic phonons resulting in thermal conductivities with magnitudes similar to amorphous materials. The guest-host interaction in clathrates continues to be of scientific interest. As a result of the interesting properties and technological promise of type I clathrates, the bulk properties of these materials have been

studied extensively using a wide range of experimental and theoretical techniques. However, to date no reports exist on the production and characterization of type I clathrate thin films. In this paper we report the first results on the growth and structural characterization of germanium-based clathrate thin films of  $\text{Ba}_8\text{Ga}_{16}\text{Ge}_{30}$  using pulsed laser deposition. One of the main advantages of laser ablation for film growth is the ability of this process to closely reproduce the target stoichiometry in the deposited film[9-11]. Therefore, laser ablation is uniquely suited for the growth of multi-component films from a single composite target such as  $\text{Ba}_8\text{Ga}_{16}\text{Ge}_{30}$ .

## EXPERIMENTAL

Bulk type I clathrate samples were prepared by mixing stoichiometric quantities of the high purity elements Ba (99%, Aldrich) or Sr (99.95%, Alfa Aesar), Ga (99.9999%, Chameleon), and Ge (99.99%, Alfa Aesar). The mixtures were placed in pyrolytic boron nitride crucibles, and sealed in fused quartz ampoules under high purity nitrogen gas at a pressure of 2/3 atm. The mixtures were heated at  $1^\circ\text{C}/\text{min}$  to form  $\text{Ba}_8\text{Ga}_{16}\text{Ge}_{30}$ , held at  $1000^\circ\text{C}$  for 24 hours, and then cooled at a rate of  $2^\circ\text{C}/\text{min}$ . For  $\text{Sr}_8\text{Ga}_{16}\text{Ge}_{30}$ , the mixture was heated at  $900^\circ\text{C}$ . The resulting products consisted of boules possessing a metallic luster, which were ground to 325 mesh (particle size  $\sim 45\ \mu\text{m}$ ). Targets for ablation were produced by hot and cold pressing procedures to a compacted density of higher than 95%.

Laser ablation system used for film growth is described in previous publications [9-11]. Three different laser wavelengths, spanning the UV (248 nm excimer), visible (frequency doubled Nd:YAG laser at 532 nm), and the IR (Nd:YAG laser fundamental at  $1.06\ \mu\text{m}$ ) were used to study the ablation characteristics of  $\text{Ba}_8\text{Ga}_{16}\text{Ge}_{30}$ . Laser pulse durations were 25 ns for the excimer and 15 ns for the Nd:YAG.

Films were grown on several different substrates that included silicon, glass, sapphire, and quartz. Substrate temperature was varied between room temperature and  $600^\circ\text{C}$ . The morphology of the films were investigated by scanning electron microscopy (SEM) while the stoichiometry was studied by EDS analysis. Structural characterization of the films was done by X-ray diffraction.

## RESULTS AND DISCUSSION

### Film morphology

The density of particulates that are ejected from the target and deposited on the film largely depends on the absorption coefficient of the target material at the wavelength of ablation and the laser fluence at the target. At the excimer laser wavelength ablation was observed for laser fluences as low as  $0.5\ \text{J}/\text{cm}^2$ . The low absorption threshold indicates high absorption coefficient of the clathrate material at this wavelength. However, at low fluences the energy of the evaporated species as well as the rate of film growth is significantly low. On the other hand, at high fluences the density of the ejected particulates become high. Fig. 1 shows SEM images of two clathrate films deposited at excimer laser fluences of  $7\ \text{J}/\text{cm}^2$  and  $3\ \text{J}/\text{cm}^2$ . The growth rates for these ablation laser fluences were  $1\ \text{\AA}/\text{pulse}$  and  $0.45\ \text{\AA}/\text{pulse}$ , respectively. Morphology of the films deposited at  $1.06\ \mu\text{m}$  and 532 nm ablation laser wavelengths at identical fluences of  $7\ \text{J}/\text{cm}^2$  are shown in Fig. 2. The growth rate at  $1.06\ \mu\text{m}$  wavelength was

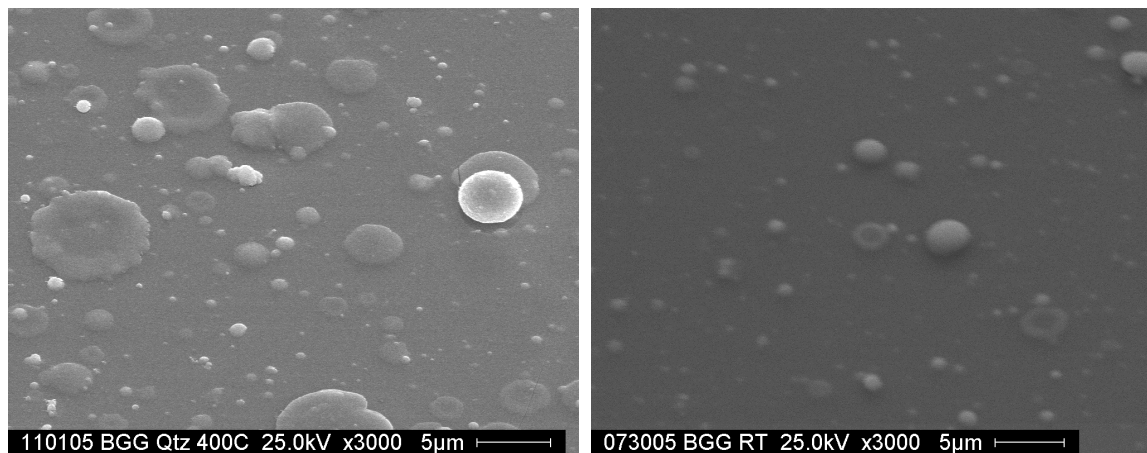


Fig. 1. SEM image of clathrate films deposited by excimer laser ablation at a wavelength of 248 nm for laser fluences of (a)  $7 \text{ J/cm}^2$ , (b)  $3 \text{ J/cm}^2$ .

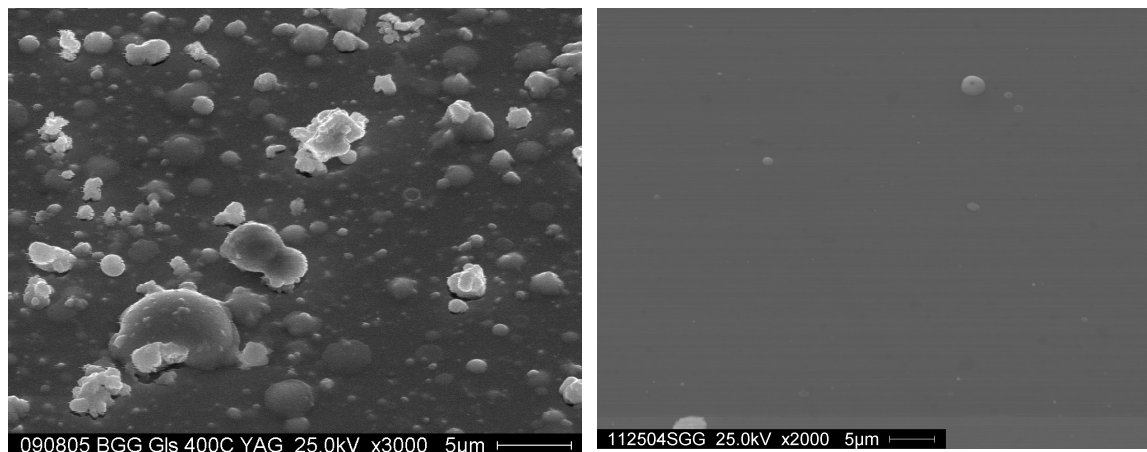


Fig. 2. SEM image of clathrate films deposited with an ablation fluence of  $7 \text{ J/cm}^2$  by (a)  $1.06 \mu\text{m}$  wavelength Nd:YAG laser, and (b)  $532 \text{ nm}$  wavelength frequency doubled Nd:YAG laser.

$1.5 \text{ \AA/pulse}$  while that for  $532 \text{ nm}$  wavelength was below  $0.1 \text{ \AA/pulse}$ . Clearly the high ablation threshold of the clathrate target at  $532 \text{ nm}$  wavelength reduced the absorption depth leading to a correspondingly low growth rate. The same reason also contributed to low particulate density.

### Film Stoichiometry

The elemental ratios of the films obtained by EDX analysis were similar for all three ablation wavelengths. Table 1 shows the stoichiometries of the films deposited on silicon, glass, sapphire, and quartz. No noticeable deviation of the stoichiometry was observed between the films deposited at room temperature and those deposited at  $400^\circ\text{C}$ . For all substrates except for silicon the elemental ratios

Substrate	Stoichiometry
Si	$\text{Ba}_8\text{Ga}_{14}\text{Ge}_{17}$
Glass	$\text{Ba}_8\text{Ga}_{16.9}\text{Ge}_{30}$
Quartz	$\text{Ba}_8\text{Ga}_{16}\text{Ge}_{30}$
Sapphire	$\text{Ba}_8\text{Ga}_{16}\text{Ge}_{28}$
Particle	$\text{Ba}_8\text{Ga}_{15.5}\text{Ge}_2$

Table 1. Film stoichiometry on different substrates

closely matched that of the target. Films on silicon appear to be Ga and Ge deficient. This deficiency resulted from the low sticking coefficients of Ga and Ge on silicon substrates. The deficiency increased with increasing substrate temperature. However, stoichiometry of films on other substrates closely resembled that of the target.

## Film Structure

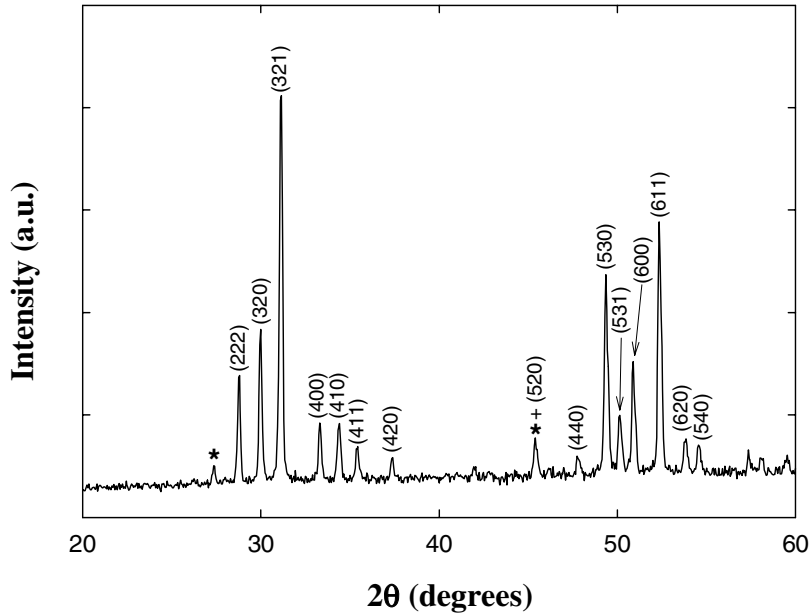


Fig. 3: X-ray diffraction pattern of the  $\text{Ba}_8\text{Ga}_{16}\text{Ge}_{30}$  target used for laser ablation. \* diamond-structure germanium as an impurity

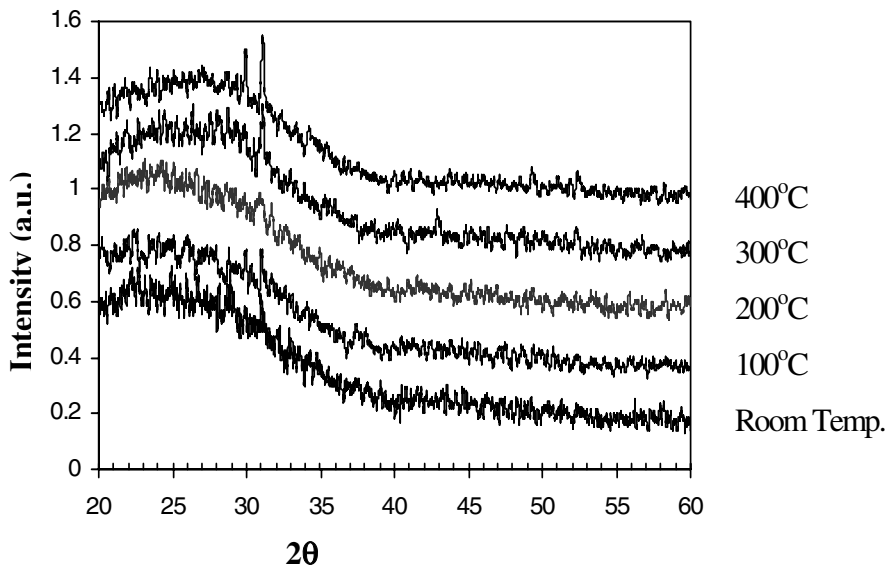


Fig. 4: X-ray diffraction patterns of clathrate films on glass substrates at temperatures from room temperature to  $400^\circ\text{C}$ .

Crystallinity of the films was determined by x-ray diffraction. The x-ray diffraction peaks produced by the clathrate target is shown in Fig. 3. Films deposited at room temperature consisted of the correct elemental ratio of type I clathrate.

However, the films were amorphous.

Fig. 4 shows the  $\theta$ - $2\theta$  scans of x-ray diffraction for films deposited on glass substrates in the temperature range from room temperature to  $400^\circ\text{C}$ . Formation of clathrate peaks corresponding to (222), (320), and (323) orientations were observed at  $400^\circ\text{C}$ . Films grown on polycrystalline quartz showed better crystallinity indicated by the well defined high intensity diffraction

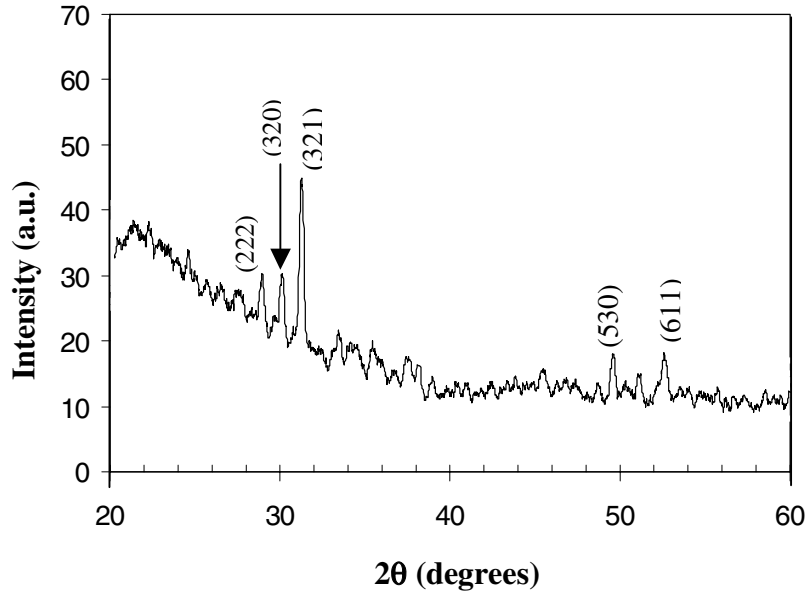


Fig. 5: X-ray diffraction patterns of a clathrate film deposited on a quartz substrates at 400°C.

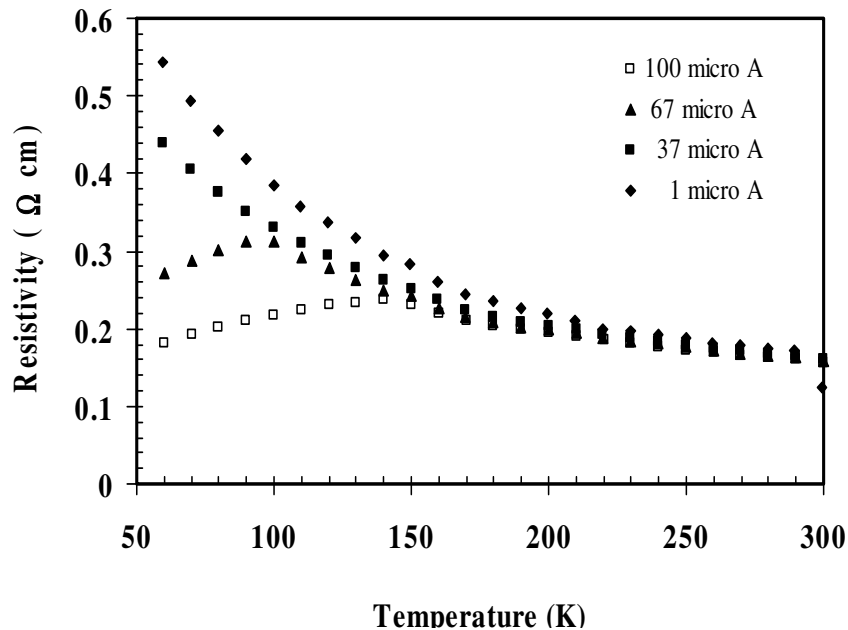


Fig. 6: Temperature and current dependence of resistivity for a laser-deposited clathrate film.

peaks (Fig. 5). Similar results were obtained for single crystal substrates.

### Electrical properties

Temperature dependent conductivity of the films was measured by a four-point probe technique. The films were mounted in a closed cycle refrigeration system that controlled the temperature in the range of 320 K to 20 K. Measurements were taken for injected currents of 1, 17, 37, 52, 67, 87, and 100  $\mu$ A. Fig. 6 shows the temperature dependence of resistivity at four different currents. Above 150 K, the films demonstrated semiconducting characteristics independent of injection current. However, at the lower values of injected currents a semiconductor-to-

metallic transition is observed as the temperature is reduced below 150 K (for an injected current of 100  $\mu$ A) and below 100 K (for an injected current of 67  $\mu$ A).

## CONCLUSIONS

The ablation threshold of the  $\text{Ba}_8\text{Ga}_{16}\text{Ge}_{30}$  target is relatively low ( $\sim 0.5 \text{ J/cm}^2$ ) for the UV and IR laser wavelengths while that for the visible laser radiation is much higher ( $> 2 \text{ J/cm}^2$ ). For all three laser wavelengths that were used in the study, stoichiometric evaporation was observed. Films deposited on most of the substrates were stoichiometric, except for silicon where low sticking coefficient led to deficiency in Ga and Ge. Films transformed from amorphous to crystalline structure above a growth temperature of  $400^\circ\text{C}$ . Growth temperatures above  $600^\circ\text{C}$  caused partial decomposition leading to the precipitation of Ge. At low injection currents films showed semiconductor behavior. The semiconductor-to-metallic transition observed as a function of decreasing temperature at high injection currents is currently being explored. Possible mechanisms for this behavior include grain-boundary effects, temperature dependent bandgap changes as well as more trivial enhanced local joule heating at high currents and high resistivities at low temperature.

## ACKNOWLEDGEMENTS

This project is partially supported by the US Department of Energy, under Grant No. DE-FG02-04ER46145 and National Science Foundation, under Grant No. DMI-0217939. MB gratefully acknowledges support from the University of South Florida Presidential Doctoral Fellowship.

## REFERENCES

1. *Semiconductors and Semimetals*, V. 69, 70, & 71, ed. T.M. Tritt, (Academic Press, 2001).
2. G.A. Slack, "New Materials and Performance Limits for Thermoelectric Cooling," *CRC Handbook of Thermoelectrics*, ed. D.M. Rowe (CRC Press, 1995), pp. 407-440.
3. G.S. Nolas, D.T. Morelli, and T.M. Tritt, *Annu. Rev. Mater. Sci.* **29**, 89 (1999).
4. C. Uher, "Skutterudites: Prospective Novel Thermoelectrics," *Semiconductors and Semimetals*, V. 69, ed. T.M. Tritt (Academic Press, 2001), pp. 139-253.
5. G.A. Slack, *Mater. Res. Soc. Symp. Proc.* **478**, 47 (1997).
6. G.S. Nolas, J.L. Cohn, G.A. Slack, and S.B. Schujman, *Appl. Phys. Lett.* **73**, 178 (1998).
7. C. Cros, M. Pouchard, and P. Hagenmuller, *J. Solid State Chem.* **2**, 570 (1970).
8. J.L. Cohn, G.S. Nolas, V. Fessatidis, T.H. Metcalf, and G.A. Slack, *Phys. Rev. Lett.* **82**, 779 (1999).
9. S. Witanachchi, K. Ahmed, P. Sakthivel and P. Mukherjee, *Applied Physics Letters*, **66**, 1469-1471 (1995).
10. P. Mukherjee, J.B. Cuff and S. Witanachchi, *J. Applied Surface Science*, **127-129**, 620 (1998).
11. P. Mukherjee, Shudong Chen, J. B. Cuff, P. Sakthivel, S. Witanachchi, *Journal of Applied Physics*, Volume **91**, Issue 4, 1828-1836, (2002).